Critical ratio between the amplitudes of two overtaking solitary water waves

Benlong Wang,[1] Jin E. Zhang,[2] Jingxin Zhang,[1] and Hua Liu[1,*]
[1]*School of Naval Architecture, Ocean and Civil Engineering, Shanghai Jiao Tong University, 200030 Shanghai, China*
[2]*SEF and SB, The University of Hong Kong, Pokfulam Road, Hong Kong*
(Received 31 May 2006; revised manuscript received 7 January 2007; published 16 March 2007)

In this paper, we study the critical ratio between the amplitudes of two overtaking solitary waves on a layer of water with uniform depth. At the center of encounter, the wave profile is fore-and-aft symmetric, but it could have a single peak or double peaks. The critical ratio separates these two regimes. At the critical point, the wave peak is flat with zero slope and curvature. We solve the full water wave problem numerically by using a fully nonlinear and highly dispersive Boussinesq model. The model is numerically justified to be a good approximation of the Euler equations for solitary waves with very large amplitude. For small amplitude water waves, our calculated critical ratio reduces to the well-known result of 3 predicted by the Korteweg–de Vries equation, a weakly nonlinear and weakly dispersive model. For large amplitude water waves, the nonlinear effect is significant; we find that the critical ratio deviates significantly from 3. For water waves with very high amplitude, e.g., 0.6 relative wave height, the critical ratio could be as large as 4. Our result suggests that higher-order nonlinear and dispersive effects are important when modeling the strong interaction between large amplitude water waves.

DOI: 10.1103/PhysRevE.75.036608 PACS number(s): 05.45.Yv, 94.05.Pt

I. INTRODUCTION

The interaction between solitary waves is an important issue in nonlinear mathematical physics. It has been studied for a few decades in fundamental science and engineering since the middle of the last century. Possible applications include tsunami waves, plasma magnetohydrodynamic waves, long waves in anharmonic crystals, and others.

Under the assumption that the nonlinear and dispersive effects are balanced, weakly nonlinear and weakly dispersive models have been developed. For example, the classical Boussinesq equations were derived for two-dimensional waves, the Korteweg–de Vries (KdV) equation was derived for unidirectional waves, and the Kadomtsev-Petviashvili (KP) equation was derived for weakly two-dimensional waves.

As a general model, the KdV equation is used to model the propagation and interaction of surface waves on a layer of water and internal waves in a shallow density-stratified fluid. The so-called inverse scattering transform for solving the KdV equation was developed by Gardner *et al.* [1] and the collision between the KdV solitary waves is shown to be elastic. The exact explicit solution of the KdV equation for multiple soliton collisions was given by Hirota [2] and was discussed in detail by Whitham [3] for the interaction between two solitons.

For the overtaking interaction between two solitary waves, they either pass through each other or remain separated throughout the encounter depending on the ratio between the amplitudes of the two solitary waves. The critical ratio separating the single-peak and double-peak regimes for overtaking solitary wave encounters was noted by Zabusky [4], proved for its existence and numerically analyzed by Lax [5], experimentally measured by Weidman and Maxworthy [6], and analytically determined by Wu [7] for the KdV equation. The critical interaction delineated by Lax [5] occurs for $\frac{1}{2}(3+\sqrt{5})<\sigma<3$, herein σ is defined as the ratio of the larger amplitude α_1 to the smaller amplitude α_2 of the incoming solitary waves.

Based on the KdV equation, it was found analytically by Wu [7] that the two crests either pass through each other or remain separated throughout the encounter according to whether the ratio of two incident solitary waves' amplitude $\sigma>3$ or $1<\sigma<3$. At the critical condition, $\sigma=3$, the single peak becomes instantaneously flattened to zero curvature.

The KdV equation and other weakly nonlinear and weakly dispersive Boussinesq equations are the first order approximation in nonlinearity and dispersiveness. In order to achieve higher accuracy in solving the water wave problem, various high order KdV models have been developed to investigate the highly nonlinear and highly dispersive effects.

By retaining high order terms, some extended KdV equations were obtained, see, e.g., [8–10]. With the third order terms, the numerical results show that after the collisions there is little change on the amplitudes of solitary waves, but a dispersive wave train occurs. This indicates that the third order equation might not be integrable.

On the other hand, the full water wave problem governed by the Euler equations could be solved numerically with modern computational techniques and increasing computational capability. Even now, the full Euler equations are still difficult to solve due to the high nonlinearity and continuous changing of the computational domain bounded by the free surface. Numerical computations of unsteady gravity waves is extensively studied in the literature. Many effective numerical models were established to simulate the highly nonlinear wave problems. Besides the boundary integral method, many accurate spectral methods were designed to solve the fully nonlinear potential problem, as in the recent works [11–13] and reviews in [14]. With these accurate numerical methods, the accuracy of various low order approximate

*Corresponding author. Email address: hliu@sjtu.edu.cn

models can be evaluated by comparing with the exact solution.

The phenomenon of forward shift of the larger wave and backward shift of the smaller wave is one of the most important characteristics of overtaking collision between two solitary waves. It attracts many interests, see, e.g., [6,15]. The kinematic property is another important aspect for the nonlinear problems. However, there are relatively few studies focusing on the critical condition. It was pointed out by Fenton and Rienecker [16] that there is a difference on the predicted critical condition between the fully potential problem and the KdV model for binary solitary wave overtaking collision. In [16], there is a slight trough between two crests at the interaction center for a ratio of $\sigma=3.142$ and $\alpha_1=0.3252$, unlike predictions from the KdV equation.

A few previous works, e.g., [5,16], have indicated the inaccuracy of the KdV theory in predicting the wave forms during the overtaking collisions. The purpose of this work is to find the variation of the critical ratio vs the wave amplitude due to the nonlinear effect in the framework of the fully nonlinear potential theory.

The fully nonlinear and highly dispersive Boussinesq (referred to herein as FNHDB) model is used to model the overtaking collision numerically. It has been demonstrated in [17] that the FNHDB model could be applied to the model wave problem accurately for weak interactions (head-on collision) between two solitary waves. Some more numerical experiments are carried out to further support the validity of the FNHDB model. With the accuracy of the FNHDB model well established, the critical condition for overtaking collision is studied.

II. FULLY NONLINEAR HIGHLY DISPERSIVE BOUSSINESQ EQUATIONS

A. Model description

Consider the flow of an incompressible, inviscid fluid with a free surface. A Cartesian coordinate system is adopted, with the x axis locating on the still-water level, and the z axis pointing upwards. The fluid domain is bounded by the seabed at $z=-h$, and the free surface at $z=\eta(x,t)$, where t stands for the time variable. The kinematic and dynamic free surface conditions are

$$\zeta_t - \tilde{w} + (\tilde{V} - \tilde{w}\zeta_x)\zeta_x = 0, \tag{1}$$

$$\tilde{V}_t + g\zeta_x + \frac{1}{2}[\tilde{V}^2 - \tilde{w}^2(1+\zeta_x^2)]_x = 0, \tag{2}$$

where

$$\tilde{V} = \tilde{u} + \tilde{w}\zeta_x. \tag{3}$$

Here $\tilde{u}$ and $\tilde{w}$ are the horizontal and vertical velocities evaluated at the free surface, g is the gravitational acceleration, and subscripts t and x denote partial derivatives. The kinematic boundary condition on a flat bottom reads

$$w_b = 0 \quad \text{at} \quad z = -h, \tag{4}$$

where w_b is the vertical velocity at the sea bed. To close the problem, the vertical distribution of the fluid velocity could be expressed by

$$u(x,z;t) = \cos[(z-\hat{z})\partial_x]\hat{u} + \sin[(z-\hat{z})\partial_x]\hat{w}, \tag{5}$$

$$w(x,z;t) = \cos[(z-\hat{z})\partial_x]\hat{w} - \sin[(z-\hat{z})\partial_x]\hat{u}, \tag{6}$$

which is an invariant form of the exact solution of the Laplace equation given by Madsen *et al.* [18]. Its original form is derived by [19]. The definition of cos and sin operators are

$$\cos(z\partial_x) = \sum_{n=0}^{\infty} (-1)^n \frac{z^{2n}}{2n!}\partial_x^{2n},$$

$$\sin(z\partial_x) = \sum_{n=0}^{\infty} (-1)^{n+1} \frac{z^{2n+1}}{(2n+1)!}\partial_x^{2n+1}.$$

From the definition in Eqs. (5) and (6), the velocity components at the free surface are $\tilde{u}=u(x,\zeta;t)$ and $\tilde{w}=w(x,\zeta;t)$ and they can be expressed in terms of $\hat{u}$ and $\hat{w}$. In the same approach, the utility velocities $\hat{u}$ and $\hat{w}$ could be used to express the velocity component at the bottom, i.e., $w_b=w(x,-h;t)$. Hence the system of fully nonlinear highly dispersive Boussinesq equations are composed by Eqs. (1)–(6). These time stepping systems are solved with the fourth order Runge-Kutta method for time integration and the seven point centered finite difference method in space. The details of the solution procedure could be found in [17].

We apply a truncated, Padé series expansion of the velocity potential about an arbitrary level $z=\hat{z}$ in the fluid layer. The Padé series truncation form of the sin and cos operators are

$$\cos(z\partial_x) = 1 - \frac{4}{9}\lambda^2\partial_x^2 + \frac{1}{63}\lambda^4\partial_x^4,$$

$$\sin(z\partial_x) = \lambda\partial_x - \frac{1}{9}\lambda^3\partial_x^3 + \frac{1}{945}\lambda^5\partial_x^5,$$

wherein $\lambda=z-\hat{z}$. In this paper, $\hat{z}$ is chosen to be the half still water depth, i.e., $\hat{z}=-h/2$, which is proved to be an accurate choice for both the linear and nonlinear properties. In the following calculations, dimensionless problems are numerically solved by choosing $h=1$ m and $g=1$ m/s^2.

B. Comments on the fully nonlinear problem

It should be pointed out that although the Boussinesq equations or model is designed for the numerical computation in this work, the numerical results are very accurate as verified for fully nonlinear and dispersive surface waves in the next subsection. The present Boussinesq equations are equivalent to the Zakharov model [20], but the system is closed in a different way. A series solution of the Laplace equation is used in the present work while an integral form is used in Zakharov's paper.

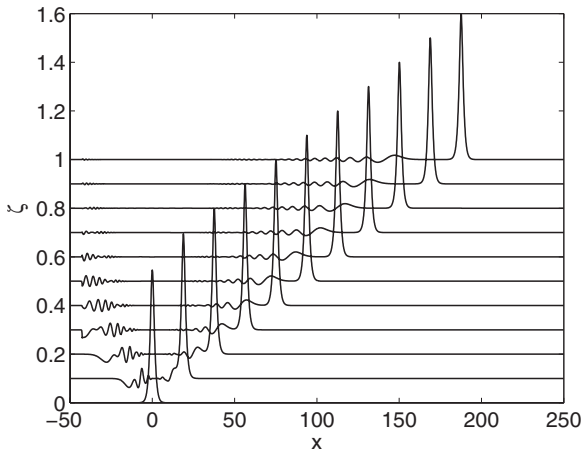

FIG. 1. Evolution of the third order Grimshaw solitary wave.

In fact, the present model gives an exact solution if infinite series are retained in Eqs. (5) and (6). In this sense, it is an asymptotical solution of the fully potential problems. Although truncations of the infinite series operators are applied, there is no approximation for the nonlinear terms. Hence it is regarded as a fully nonlinear model.

The truncation affects the dispersive character of the wave model. The accuracy of the Padé series is verified by [17,21,22] for fully nonlinear and highly dispersive problems. The truncation of the infinite Taylor series approaches the exact solution for long waves but leaves the approximation for short waves. From the Fourier analysis of the linear dispersion relation and nonlinear transfer function, the relative error is neglectable for $kh \leqslant \pi$ when the Padé series truncation is used, where k is the wave number and h is the water depth. The wavelength of the waves with $kh=\pi$ is about two times the water depth, which is much shorter than the general solitary waves. For long waves there is almost no loss of accuracy comparing the fully nonlinear and fully dispersive problems. Even for extremely high solitary waves, e.g., $\alpha=0.6$, the wavelength is about 10, which is still much longer than the limit of the application range.

Compared with the weakly nonlinear and weakly dispersive models, such as the KdV equation and the Camassa-Holm equation [23], the present Boussinesq model is fully nonlinear and highly dispersive. It is a much better approximation of the Euler equations. Furthermore, the present model provides velocity distribution in addition to surface elevation, therefore it provides a deeper insight about the collisions.

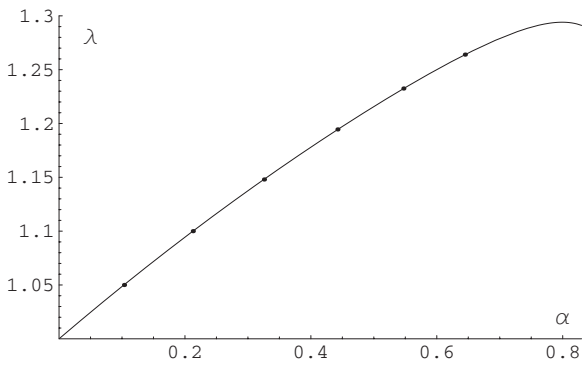

FIG. 2. Comparison on the phase celerity between FNHDB and the Jonsson's rational-function approximation.

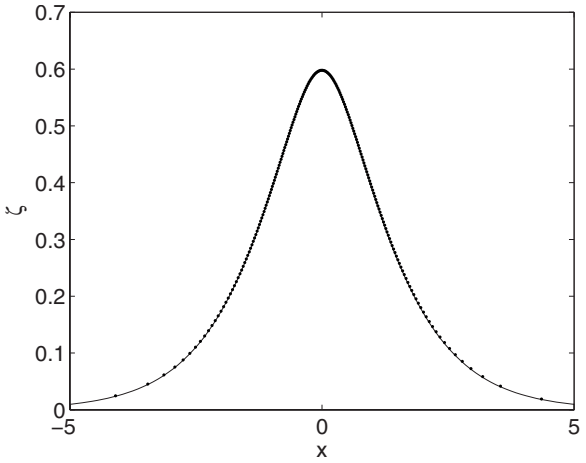

FIG. 3. Comparison on the solitary wave profiles between Wu [13] (dots) and FNHDB (solid line).

C. Verification

For the time stepping problems, a proper initial condition is necessary. However, no explicit analytical solitary solution to the FNHDB model is known yet. Hence we need to obtain the actual wave profile and velocity from the evolution of an arbitrary approximate initial condition numerically.

An approximate initial condition, the third order Grimshaw's solitary wave solution, is proposed along the wave flume. Due to the inconsistence between the initial wave and the FNHDB model, the solitary wave will deform and trailing waves will separate from the major part of the wave. In general, both the wave amplitude and profile will change. To obtain the initial condition for a desired amplitude solitary wave, several runs are needed. Propagating for a long distance, a pure and steady solitary wave satisfying the FNHDB model will be formed. In this sense, the numerical solitary wave solution to the FNHDB model is obtained with self-balance of nonlinearity and dispersion. After discarding the trailing waves, the velocity and surface elevation are saved for further studies.

The temporal evolution history of the third order Grimshaw's solitary wave governed by the FNHDB model is shown in Fig. 1. The free surface elevation is uplift for 0.1 in the vertical direction and the time interval is 15 s. As displayed in Fig. 1, the initial third order Grimshaw's solitary wave of height 0.5461 develops into a solitary wave of height 0.6 satisfying the FNHDB model after a long distance evolution.

After the steady wave profile and velocity field are obtained, various studies can be performed. The celerity estimated from the numerical solution of the FNHDB model is 1.2507 for steady wave amplitude $\alpha_1=0.6$. Comparing the rational-function approximation formulation [24], the relative error is about 0.1%. With the same procedure, the other

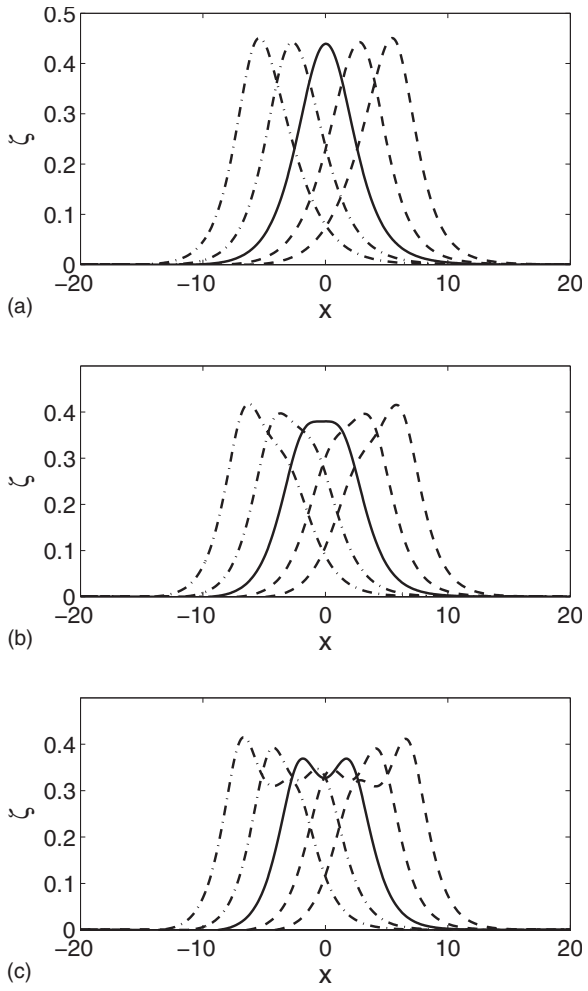

FIG. 4. Time evolution of two overtaking solitary waves, for $\alpha_1=0.6$, and $\alpha_2=0.1$ in (a), 0.1503 in (b), and 0.2 in (c), with time interval $\Delta t=2$ s. Dashed-dotted lines: wave surface profiles before the encounter; solid lines: wave surface profiles at the center of encounter; dashed lines: wave surface profiles after the encounter.

wave's celerity is calculated and shown in Fig. 2. Keeping the Courant number equal to 0.5, the spatial grid sizes vary from 0.2 to 0.02 according to the wave amplitudes in these runs. Good agreements are found for both the small and large amplitude waves. Moreover, the solitary waves' reflections from the vertical wall are calculated in [17] using the present FNHDB model and the numerical results agree well with others. The reflection of a solitary wave from a vertical wall mimics the head-on collision, which is the kind of weak interaction. All these verifications guarantee the effectiveness of the proposed model in simulating the strong interactions between binary solitary waves overtaking collision.

Before ending the section of validation, a critical comparison on the profiles of the FNHDB model against Wu's result [13] is conducted, as shown in Fig. 3. Herein the wave amplitude takes the value of $\alpha=0.597\,97$. As we know, the accuracy of the surface profile is a good manuscript of the numerical model when considering the nonlinear and dispersive characteristics. There is almost no difference between the numerical results of the FNHDB model and Wu's profile, which means the FNHDB model is a very good approximation of the Euler equations and it is an accurate model to simulate solitary waves, even for extremely high nonlinear solitary waves.

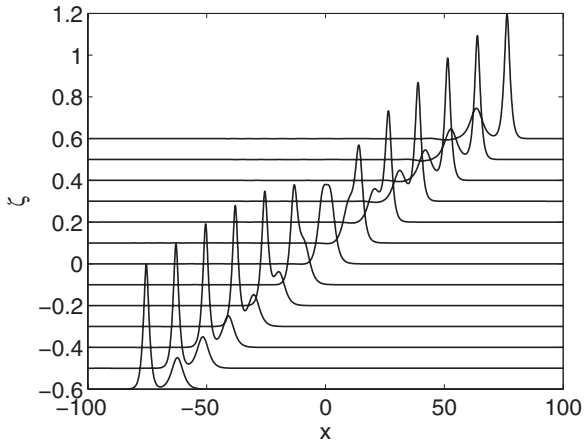

FIG. 5. Time evolution of two overtaking solitary waves with $\alpha_1=0.6$ and $\alpha_2=0.1503$.

III. OVERTAKING COLLISIONS

A. Critical ratio

The overtaking collisions between two solitary waves are numerically simulated to find the critical ratio. The critical ratio is the ratio between the amplitudes of the two incident waves, $\sigma=\alpha_1/\alpha_2$, for which the curvature of the surface elevation is zero at the center of encounter during the overtaking collision.

Keeping the amplitude of large solitary wave, α_1, fixed, a few combinations with several relative small solitary waves of amplitude α_2 around the critical condition are simulated for the overtaking collision. Whether the two crests pass through each other or remain separated can be identified by evaluating the curvature of the free surface elevation at the center of encounter. When the two incoming solitary waves satisfy the critical condition, the curvature of the free surface is zero at the center.

The initial conditions were taken to be two waves placed adjacent to each other with a distance long enough to ensure that the superposition effect is not introduced, as verified by preliminary numerical tests.

For $\alpha_1=0.6$, calculations with various α_2 are carried out. The numerical results for $\alpha_2=0.1$, 0.2, and 0.1503 are shown in Fig. 4. The time interval between adjacent surface elevations is 2 s. The dash-dot lines are surface elevations before the encounter instant, and the dash lines are after the encounter instant. At the encounter instant, shown by the solid line, there are two class profiles: there is only one peak for $\alpha_2=0.1$ and double peaks for $\alpha_2=0.2$. The separation of these two profiles is the critical condition, i.e., $\alpha_2=0.1503$ for $\alpha_1=0.6$. A zooming-out time evolution is shown in Fig. 5 for two incoming waves satisfying the critical condition. The free surface elevation is uplift for 0.1 in the vertical axis and the time interval is 10 s for two adjoining time instants.

At the center of encounter, the detailed geometrical properties, such as surface slope and curvature, are shown in Fig.

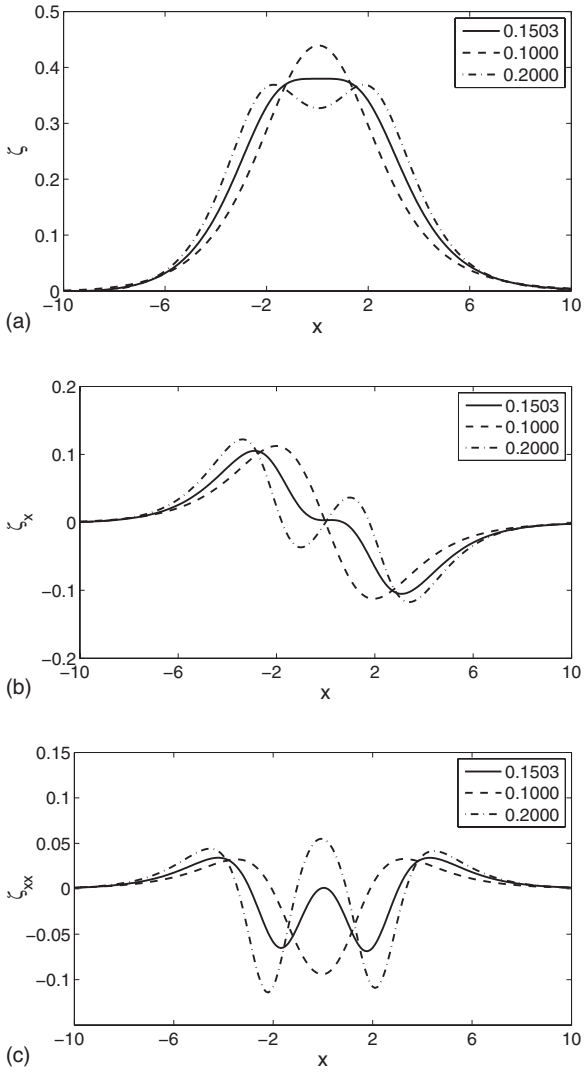

FIG. 6. The wave profiles at the center of encounter of two overtaking solitary waves with $\alpha_1=0.6$, $\alpha_2=0.1$, 0.2, and 0.1503. Top panel (a): free surface elevation; middle panel (b): slope of the surface elevation; bottom panel (c): curvature of the surface elevation.

6. Both the slope of the surface ζ_x and the curvature ζ_{xx} are zero at the peak, which satisfies the critical condition.

With the same procedure, other combinations are conducted. The numerical results for the critical conditions are listed in Table I for waves of both small amplitude and large amplitude. For very weak nonlinear waves, e.g., $\alpha_1<0.1$, the wavelength becomes very long and the separation of the large amplitude wave and the small one needs a much longer distance. The critical ratio approaches 3, the value predicted by the KdV equation for small amplitude waves. For extremely small waves, e.g., $\alpha_1=0.06$ and $\alpha_2=0.0199$ satisfying the critical condition, the minimal surface elevation during the encounter is 0.0399, which is very close to the value $\alpha_1-\alpha_2$ predicted by the KdV model. For large amplitude waves, the critical condition significantly deviates from the weakly nonlinear and weakly dispersive model. When $\alpha_1=0.6$, the critical ratio is closer to 4. The minimal surface elevation during the encounter is 0.3801, which is much smaller than the value of $\alpha_1-\alpha_2=0.4497$ predicted by the KdV theory.

TABLE I. Critical ratios for overtaking collision vs a list of values for α_1.

α_1	α_2	σ
0.0600	0.0199	3.012
0.1032	0.0329	3.137
0.2121	0.0648	3.273
0.3255	0.0944	3.448
0.4422	0.1211	3.651
0.5469	0.1412	3.873
0.6000	0.1503	3.992
0.6444	0.1570	4.104

B. Velocity field

Besides the free surface elevation ζ and velocity components $\hat{u}$ and $\hat{w}$, the velocity field could be constructed by using Boussinesq formulas (5) and (6). The velocity field is shown in Figs. 7 and 8.

For the overtaking collision, the horizontal velocity decreases along the vertical z axis from the free surface $z=\zeta$ to bottom $z=-1$ within a range of x, e.g., $x\in(-3.55,3.55)$ in Fig. 9 and $x\in(-3.11,3.11)$ in Fig. 10. Outside these regions, the horizontal velocity increases from surface to bottom, hence the maximum horizontal velocity occurs at the bottom. This property holds for arbitrary solitary waves in the framework of the fully nonlinear and highly dispersive theory.

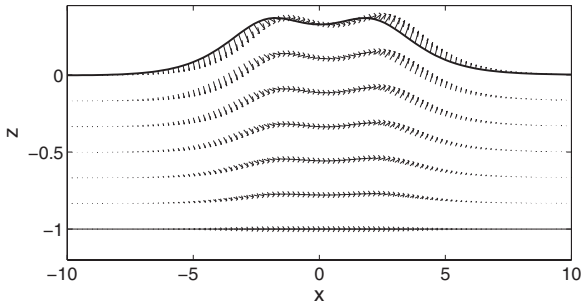

FIG. 7. Velocity field at the center of encounter for $\alpha_1=0.6$ and $\alpha_2=0.2$.

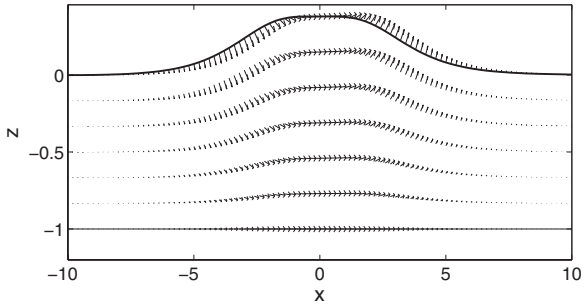

FIG. 8. Velocity field at the center of encounter for $\alpha_1=0.6$ and $\alpha_2=0.1503$.

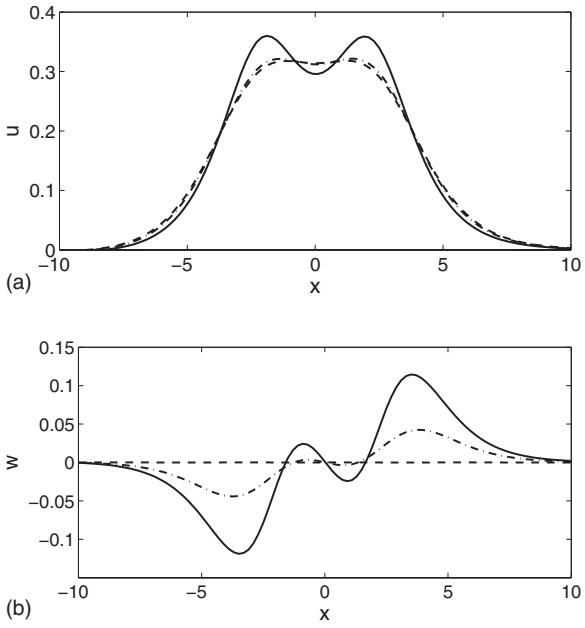

FIG. 9. Top panel (a): horizontal velocity at free surface (solid line), $\hat{z}$ (dashed-dotted line), and bottom (dashed line); bottom panel (b): vertical velocity at free surface (solid line), $\hat{z}$ (dashed-dotted line), and bottom (dashed line).

A typical computed velocity distribution is shown in Fig. 11 for a single solitary wave with amplitude $\alpha=0.6$. Since the solitary wave is a long wave, the first order approximation of velocity distribution could be used to explain the distribution property of the velocity field. Neglecting the higher order dispersive terms, the Boussinesq formula (5) could be simplified as

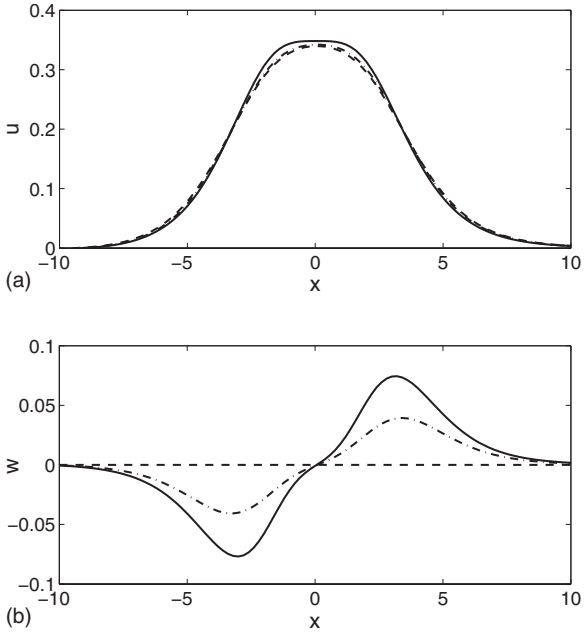

FIG. 10. Top panel (a): horizontal velocity at free surface (solid line), $\hat{z}$ (dashed-dotted line), and bottom (dashed line); bottom panel (b): vertical velocity at free surface (solid line), $\hat{z}$ (dashed-dotted line), and bottom (dashed line).

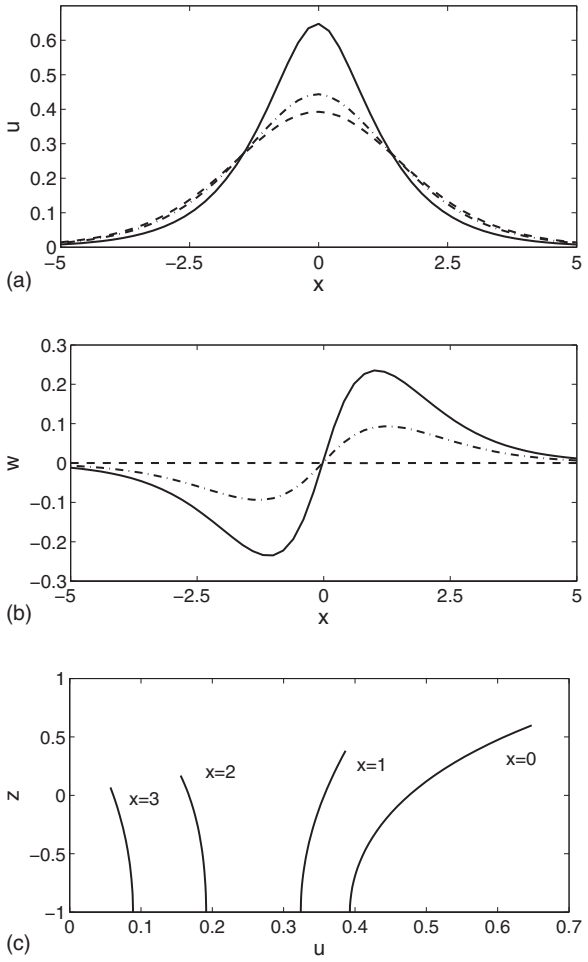

FIG. 11. Velocity distributions for $\alpha=0.6$. Horizontal velocity [top panel (a)] and vertical velocity [middle panel (b)] at free surface (solid line), $\hat{z}$ (dashed-dotted line), and bottom (dashed line); bottom panel (c): horizontal velocity distributions along z axis at different locations.

$$u(x,z,t) = \hat{u}(x,t) + (z-\hat{z})\hat{w}_x(x,t) + \cdots . \tag{7}$$

Taking $\hat{u}(x,t)$ as a reference, the velocity reads $\tilde{u}(x,t) = \hat{u}(x,t) + (\zeta+0.5)\hat{w}_x(x,t)$ at free surface and $u_b(x,t) = \hat{u}(x,t) - 0.5\hat{w}_x(x,t)$ at the bottom. Within the interval of the two extremum values of $\hat{w}$, $\hat{w}_x$ has positive value, as shown in Fig. 11, thus the velocity at the level above $\hat{z}$ is higher than $\hat{u}$ while the velocity below $\hat{z}$ is lower than $\hat{u}$. Since ζ is positive, $\tilde{u}-\hat{u}$ is larger than $\hat{u}-u_b$. Outside this interval, the value of $\hat{w}_x$ is negative. Consequently, the horizontal velocity distribution along the vertical direction has an opposite trend. In addition, the absolute value of $\hat{w}_x$ around the peak is larger than that in the far field, therefore the horizontal velocity changes more rapidly near the peak but more gently in the far field.

C. Comparison with other high order theories

Including the second order terms, the extended KdV equation reads

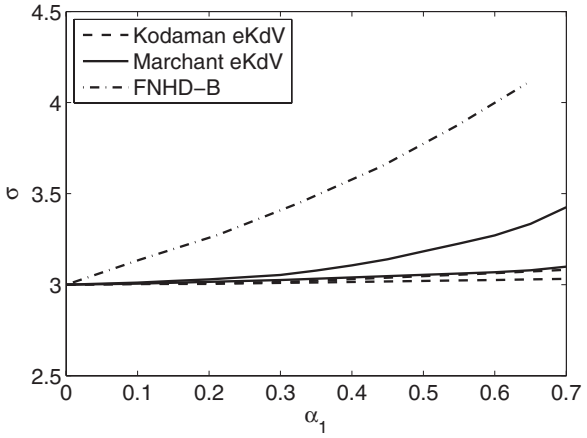

FIG. 12. Comparison on critical ratios between two extended KdV models and the FNHDB model.

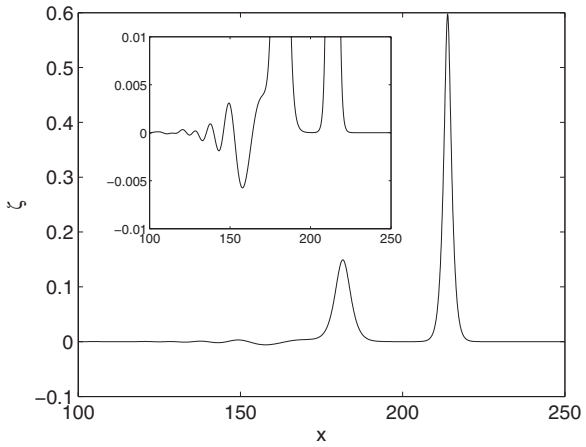

FIG. 13. Trailing waves at 170 s after encounter of the binary solitary waves collision, $\alpha_1=0.6$.

$$\zeta_t + 6\zeta\zeta_x + \zeta_{xxx} + \alpha c_1\zeta^2\zeta_x + \alpha c_2\zeta_x\zeta_{xx} + \alpha c_3\zeta\zeta_{xxx} + \alpha c_4\zeta_{xxxxx} = 0, \quad (8)$$

where α is a dimensionless measurement of the wave amplitude. For the case of surface waves in shallow water, the coefficients are

$$c_1 = 1, \quad c_2 = \frac{2}{3}, \quad c_3 = \frac{1}{3}, \quad c_4 = \frac{1}{30}$$

derived by Kodaman [9] and

$$c_1 = -1, \quad c_2 = \frac{23}{6}, \quad c_3 = \frac{5}{3}, \quad c_4 = \frac{19}{60}$$

derived by Marchant and Smyth [10].

The asymptotical solution can be obtained by transforming the extended KdV (eKdV) equation to the KdV equation as discussed in [25]. There are two branches for each eKdV model in Fig. 12. This is because the parameter α in Eq. (8) cannot be uniquely determined for a binary solitary waves system. Each branch corresponds to either α_1 or α_2, and the critical conditions should lie somewhere between the two branches. Including the second order terms, the critical condition increases and is larger than 3, while still much smaller than the value predicted by the FNHDB model.

After a long time evolution, herein 170 s after the encounter for $\alpha_1=0.6$, a small trailing wave separates from the solitary waves, as observed in Fig. 13. To eliminate the influence of numerical dispersion, either the small amplitude wave or the large wave is run separately and no trailing wave is found. This implies that the trailing wave is generated during the overtaking collision. In the inset, the vertical scale is magnified to observe the dispersive trailing waves generated by the interaction. The overtaking collision of solitary waves is perfectly elastic for the KdV model. From the computational results of the FNHDB model, the overtaking collision is nearly elastic, which agrees with other numerical results of high order KdV models.

IV. CONCLUSIONS

By numerically solving the fully nonlinear and highly dispersive Boussinesq equations, it is found that the critical ratio is related to the leading solitary wave amplitude for overtaking collision. For an extremely small wave, the critical ratio approaches 3, which indicates that the various KdV models or bidirectional long wave models give reasonably correct predictions. With the increasing of the wave amplitude, the critical ratio increases and is significantly different from 3. For extremely strong nonlinear waves, e.g., $\alpha_1 \approx 0.6$, the critical ratio reaches the magnitude of 4 and the collision is nearly elastic.

ACKNOWLEDGMENTS

The research has been supported by the National Science Foundation of China (Grant Nos. 10172058 and 10572093), the Special Fund for PhD Programs of the Education Ministry of China (Grant No. 2000024817), and the Research Grants Council of Hong Kong.

[1] C. Gardner, J. Green, M. Kruscal, and R. Miura, Phys. Rev. Lett. **19**, 1095 (1967).
[2] R. Hirota, Phys. Rev. Lett. **27**, 1192 (1971).
[3] G. Whitham, *Linear and Non-linear Waves* (Interscience, New York, 1974).
[4] N. Zabusky, *Nonlinear Partial Differential Equations* (Academic Press, New York, 1967).
[5] P. Lax, Commun. Pure Appl. Math. **21**, 467 (1968).
[6] P. Weidman and T. Maxworthy, J. Fluid Mech. **85**, 417 (1978).
[7] T. Wu, Acta Mech. Sin. **11**, 289 (1995).
[8] Q. Zou and C. Su, Phys. Fluids **29**, 7 (1986).
[9] Y. Kodaman, Phys. Lett. **107A**, 245 (1985).
[10] T. Marchant and N. Smyth, J. Fluid Mech. **221**, 263 (1990).
[11] A. Dyachenko, E. A. Kuznetsov, M. Spector, and V. Zakharov,

Phys. Lett. A **221**, 73 (1996).
[12] W. Choi and R. Comassa, J. Eng. Mech. **125**, 756 (1999).
[13] T. Wu, Acta Mech. Sin. **21**, 1 (2005).
[14] W. Tsai and D. Yue, Annu. Rev. Fluid Mech. **28**, 249 (1996).
[15] R. Mirie and C. Su, J. Fluid Mech. **115**, 475 (1982).
[16] J. Fenton and M. Rienecker, J. Fluid Mech. **118**, 411 (1982).
[17] P. Madsen, H. Bingham, and H. Liu, J. Fluid Mech. **462**, 1 (2002).
[18] P. Madsen, D. Fuhrman, and B. Wang, Coastal Eng. **53**, 487 (2006).
[19] L. Rayleigh, Philos. Mag. **5**, 257 (1876).
[20] V. Zakharov, J. Appl. Mech. Tech. Phys. **9**, 190 (1968).
[21] P. Madsen and H. Schäffer, Philos. Trans. R. Soc. London, Ser. A **356**, 3123 (1998).
[22] P. Madsen, H. Bingham, and H. Schäffer, Proc. R. Soc. London, Ser. A **459**, 1075 (2003).
[23] R. Camassa and D. D. Holm, Phys. Rev. Lett. **71**, 1661 (1993).
[24] O. Jonsson, P. Thorup, and H. Tamasauskas, Ocean Eng. **27**, 511 (2000).
[25] T. R. Marchant, Phys. Rev. E **59**, 3745 (1999).